Steel and Composite Structures, *Vol. 24, No. 4 (2017) 455-465*
DOI: https://doi.org/10.12989/scs.2017.24.4.455

Concrete-filled rectangular hollow section X joint with Perfobond Leister rib structural performance study: Ultimate and fatigue experimental Investigation

Yongjian Liu [1], Zhihua Xiong*[2], Yuncheng Feng [2] and Lei Jiang [1]

[1] *School of Highway, Chang'an University, Xi'an 710064, China*
[2] *CCCC First Highway Consultants Co., Ltd., Xi'an 710075, China*

(*Received November 24, 2016, Revised March 29, 2017, Accepted April 26, 2017*)

Abstract. This paper presents a series of ultimate and fatigue experimental investigation on concrete-filled rectangular hollow section (CRHS) X joints with Perfobond Leister rib (PBR) under tension. A total of 15 specimens were fabricated, in which 12 specimens were tested under ultimate tension and 3 specimens were investigated in fatigue test. Different parameters including PBR stiffening, brace-to-chord ratio (β) and inclined angle (θ) were considered in the test. Each joint was tested to failure under tension load. Obtained from test result, PBR was found to improve the tension strength and fatigue durability of CRHS joint substantially. Concrete dowel consisted by PBR and concrete inside the chord stiffened the joint, which leaded to a combination failure mode of punching shear and chord plastification of CRHS joint under tension. Finite element analysis validated the compound failure mode. Stress concentration on typical spot of CRHS joint was mitigated by PBR which was observed from fatigue test. Initial fatigue crack presented in CRHS joint with PBR also differentiated with the counterpart without PBR.

Keywords: concrete-filled rectangular joint; perfobond leister rib; experimental investigation; fatigue; concrete dowel

1. Introduction

As the increased use of structure with concrete-filled rectangular hollow section (CRHS) in the construction of infrastructure such as bridge (Liu *et al*. 2015, Hanswille 2011), several of tests and theoretical works have been carried out to learn the strength of CRHS joint. Concrete filling is an effective stiffening method for rectangular hollow section (RHS) joint's compression strength improvement which has been studied by Packer (1995). CRHS T, Y, X joint failure mode in compression regarding variable β have been given (Packer *et al*. 2010). From the previous research, CRHS joint has a much improvement in compression strength than the hollow counterpart, however, it rarely helps with the tension strength. In truss bridge, typical K and N type joint is loaded in a state which one brace is in compression and the other is in tension. Perfobond Leister rib (PBR) welded in chord face with concrete-filled has been found to be a significant alternative to increase the ultimate tension strength by Xiong *et al*. (2014).

Perfobond Leister (PBL) was invented and applied in construction in German initially. Recently, composite dowel consisting of perfobond leister with clothoid strip and concrete has been preferred in both highway and railway composite bridge in German (Seidl *et al*. 2013, Tue and Küchler 2006). Composite dowel applied in bridge deck was demonstrated in Fig. 1. Composite dowel design concept for ultimate limit state and fatigue limit state was given by Feldmann *et al*. (2015). Composite dowel with ultra-high performance concrete (UHPC) fatigue performance was investigated by Gallwoszus and Classen (2015), which indicated its fatigue lifetime estimation under cyclic pull out loading. Push-out experiments of PBL connector were carried out, strength equations were regressed based on the tests (Ahn *et al*. 2010, Zheng *et al*. 2016). Eurocode 4's code provision about PBL was verified by Machacek and Cudejko (2009) through 3 test composite beams using PBL. Cândido-Martins *et al*. (2010) carried out experiments on PBL shear resistance with consideration for the interaction effect between two PBL shear connector side by side.

For the truss bridge, fatigue strength is another key point which should be evaluated in design. Several research attentions have been concentrated in concrete-filled circular hollow section (CHS) joint's fatigue strength and fatigue life evaluation (Cui and Shao 2015). Concrete filling has been validated to reduce localized stress at the weld toe of the CHS joint by Sakai *et al*. (2004) and Schumacher A. *et al* (2006). Schumacher *et al*. (2009) has demonstrated the effect of size on the fatigue strength of welded tubular joints (CHS) by large-scale tests. The size correction factor integrated into the S–N design curve of the specification has been found not to represent this significant effect justly. In view of the size effect, a more coherent definition of the size effect, whereby the influences of different joint parameters and dimensions are accounted for individually, is suggested. Fatigue life of welded joint subjected to bending was studied by Baik *et al*. (2011) and Xiao *et al*.

*Corresponding author, Ph.D.,
E-mail: xiongzhihua_2013@126.com

ISSN: 1229-9367 (Print), 1598-6233 (Online)

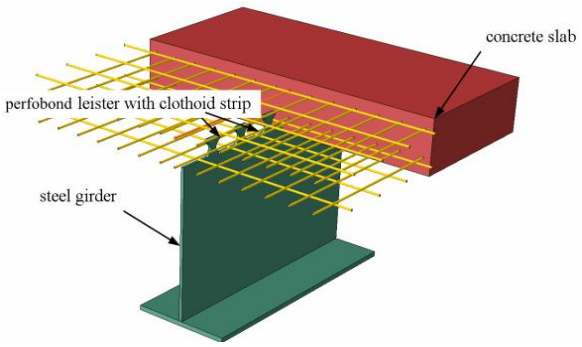

(a) General configuration

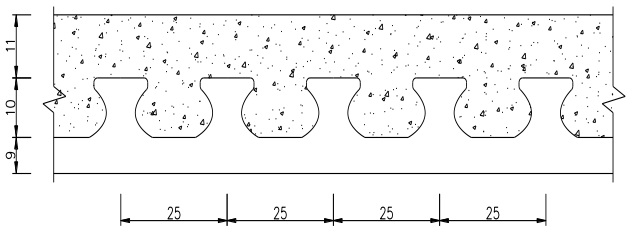

(b) Composite dowels detail (unit: cm)

Fig. 1 Perfobond leister with clothoid strip used in composite bridge in Germany

(2012) through test and linear fracture mechanics analysis.

The aforementioned tests were all conducted either on tubular joints or on PBL in concrete slab. In this paper PBR was installed in chord face to improve CRHS joint's tension strength and fatigue performance, which was validated in the following ultimate and fatigue experiments.

2. Experimental setup

2.1 Test specimens

A total of 15 specimens were tested by applying tensile force and fatigue load, in which 12 specimens were applied

Table 1 Details of test specimens

No.	Chord (h_0×b_0×t_0)(mm)	Brace (h_1×b_1×t_1)(mm)	β (b_1/ b_0)	θ^0	PBR	Note
J1	120×80×3	60×60×3	0.75	60	○	
J2	120×80×3	60×60×3	0.75	60	○	
J3	120×80×3	60×60×3	0.75	60	×	
J4	120×80×3	50×50×3	0.625	60	○	
J5	120×80×3	50×50×3	0.625	60	×	
J6	120×80×3	50×50×3	0.625	60	○	○: with PBR;
J7	120×80×3	60×60×3	0.75	90	○	×: without PBR;
J8	120×80×3	60×60×3	0.75	90	○	××: hollow joint without PBR;
J9	120×80×3	50×50×3	0.625	90	○	J1-J12 were for ultimate tests,
J10	120×80×3	50×50×3	0.625	90	○	J13-J15 were for fagitue tests
J11	120×80×3	60×60×3	0.75	60	××	
J12	120×80×3	50×50×3	0.625	60	××	
J13	120×80×3	50×50×3	0.625	60	○	
J14	120×80×3	60×60×3	0.75	60	×	
J15	120×80×3	60×60×3	0.75	60	○	

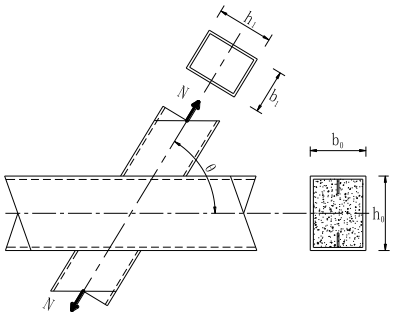

Fig. 2 General configuration of CRHS joint

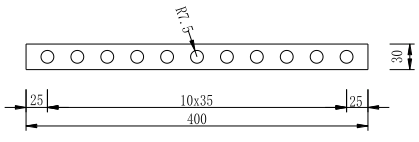

Fig. 3 PBR configuration (mm)

Fig. 4 Chord and PBR fabrication

ultimate tensile load and 3 specimens were applied fatigue load. Table 1 summarized the characteristics of the test joints. The general detail of the joint was shown in Fig. 2. All specimens were fabricated with brace plates fully welded to the chord. Joint's plate thickness including PBR were 3 mm. Radius of 7.5 mm hole was aligned with a distance of 35 mm in PBR as shown in Fig. 3. PBR was welded along the longitudinal direction of the chord with a length of 400 mm. Chord was made by welding the two folded plate with PBR together as shown in Fig. 4. On top of the joint specimens a cover plate was welded to the brace end with a nominal diameter of 32 mm rebar. The weld procedure was performed by CO_2 arc-welding. The leg size of welded joint was about 4 mm. After welding, each joint was hammered and burnished to avoid significant residual stress and defects.

2.2 Material property

All hollow joints including both brace and chord members were fabricated by Chinese Standard Q235 steel. Tensile coupon tests were conducted to determine the material mechanical properties. The coupon specimens were fabricated according to the recommendations of the Chinese code of metallic material test. The tensile coupon test was shown in Fig. 7. The material properties of concrete were determined from the compressive concrete cubes tests. A total of 6 standard concrete cubes with the nominal length of 150 mm according to Chinese Code were poured and prepared. The material properties of the standard cubes were listed in Table 2, in which the mean value of the concrete strength was 50.3 MPa.

2.3 Test rig and procedure

The specimen for ultimate tension test was installed in the test rig as shown in Fig. 8. Each brace end was provided with a rebar. The top rebar was gripped by the actuator and the bottom rebar to the strong base of the test rig. In each of the ultimate tension tests, the joint was loaded axially through the brace to failure by displacement-controlled quasi-static loading. Displacement transducer was installed in the actuator. Strain gauges were set both on the chord and brace, whose positions and tags were demonstrated in Fig. 5.

The specimen for fatigue test was installed in the test rig as shown in Fig. 6. The mode of loading was similar with ultimate test. The brace was subjected to a cyclic axial force with constant amplitude from tension to tension. The fatigue load frequency was 7 Hz. The fatigue load shifted between the P_{max} and P_{min} as listed in Table 3.

Table 2 Material properties of concrete

No.	Compressive cube strength (MPa)	Mean value (MPa)
1	50.36	50.25
2	49.94	
3	51.30	
4	47.98	
5	50.64	
6	51.28	

3. Result and discussion

3.1 Axial load-displacement response

Table 4 summarized the ultimate test results, where N_u and Δ_u were the ultimate load and its corresponding

Table 3 Fatigue load parameter

No.	P_{min} (kN)	P_{max} (kN)	P_{mid} (kN)	$\Delta\sigma_n$ (MPa)	Stress ratio, R
J13	5	30	17.5	41.7	0.17
J14	5	40	22.5	48.6	0.125
J15	5	40	22.5	48.6	0.125

Fig. 8 Test rig for fatigue

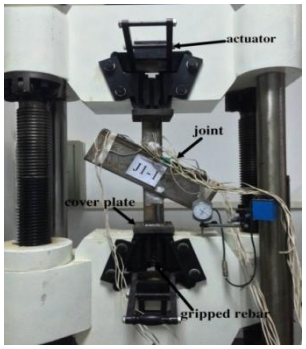

Fig. 5 Test rig for ultimate tension

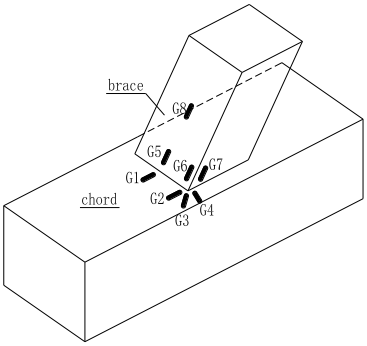

Fig. 6 Arrangement of strain gauges

Fig. 7 Coupon test

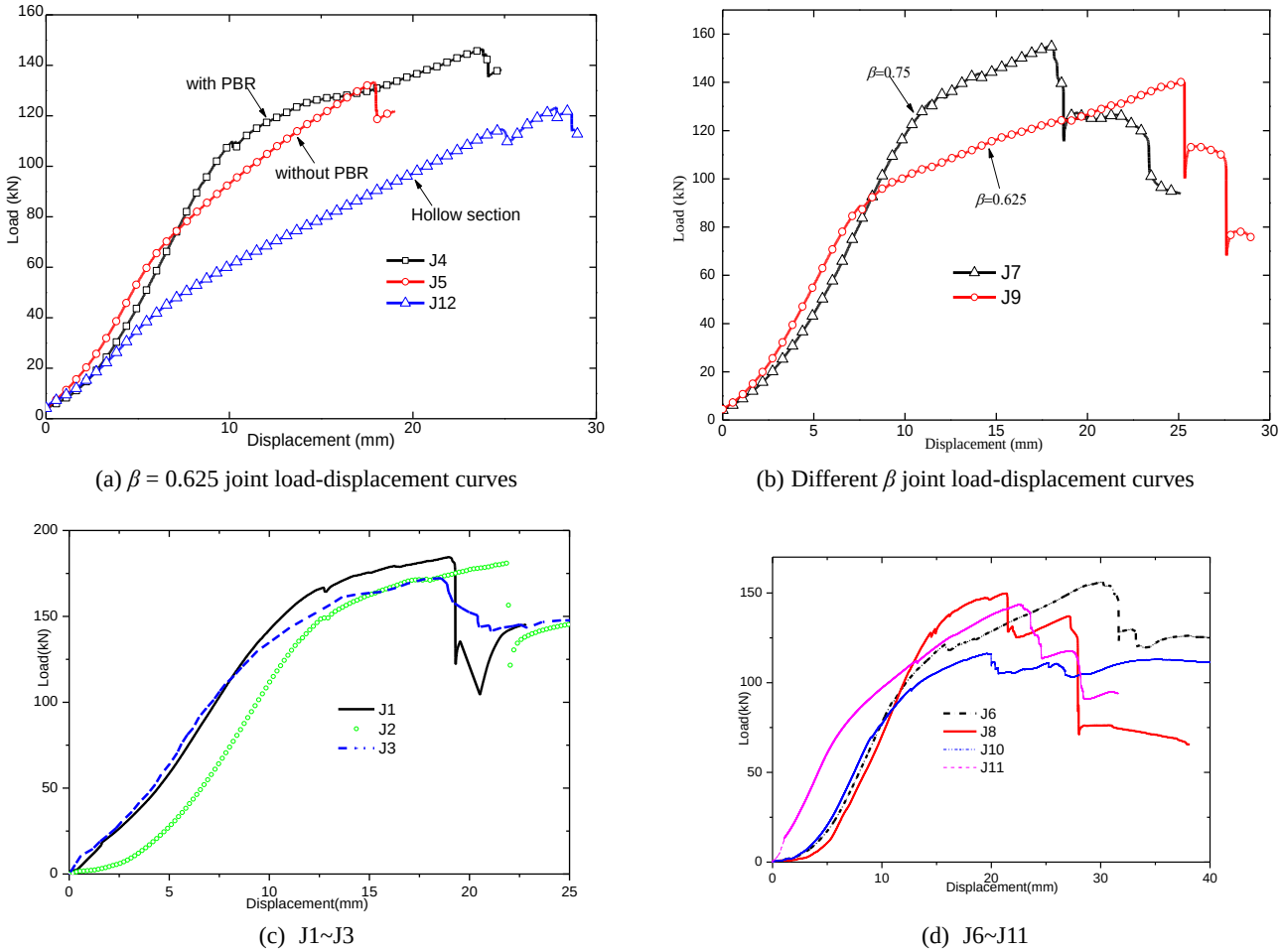

(a) β = 0.625 joint load-displacement curves

(b) Different β joint load-displacement curves

(c) J1~J3

(d) J6~J11

Fig. 9 Test joints load-displacement curves

Table 4 Test joint ultimate load and corresponding displacement

No.	β	θ^0	N_u (kN)	Δ_u (mm)	PBR	Note
J1	0.75	60	184.5	18.9	○	
J2	0.75	60	181.0	19.4	○	
J3	0.75	60	172.2	18.6	×	
J4	0.625	60	146.4	23.8	○	
J5	0.625	60	133.3	17.9	×	
J6	0.625	60	156.2	27.1	○	○: with PBR;
J7	0.75	90	155.0	18.0	○	×: without PBR;
J8	0.75	90	149.7	17.7	○	××: hollow joint without PBR;
J9	0.625	90	140.3	25.2	○	
J10	0.625	90	116.2	18.6	○	
J11	0.75	60	143.7	22.6	××	
J12	0.625	60	123.3	27.8	××	

displacement respectively. As shown in Table 4, in terms of ultimate tension strength, the CRHS joint with PBR tensile performance was better than the joint without PBR in general. All the joints' load-displacement curves were plotted in Fig. 9. Within the initial 10 mm, tangent modules of curves remained still and the joints were in elastic stage. As the displacement increased, the stiffness of the joint with PBR degraded, which mainly attributed to two reasons: (1)yielding of material; (2) the interaction between PBR and the concrete. While for the joint without PBR, there was rarely reduction of stiffness till the peak load. The joint with PBR reached the peak load with chord face plastification

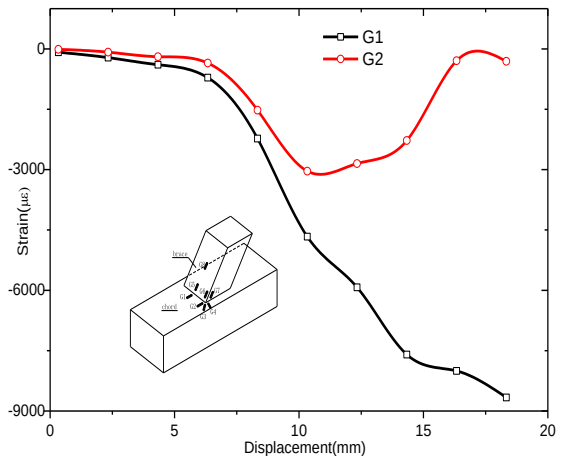

(a) J2 chord

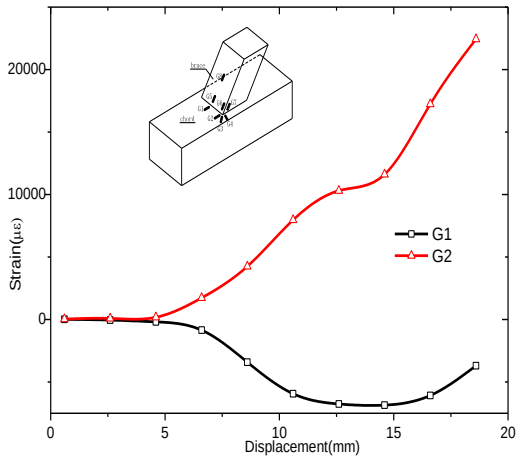

(b) J3 chord

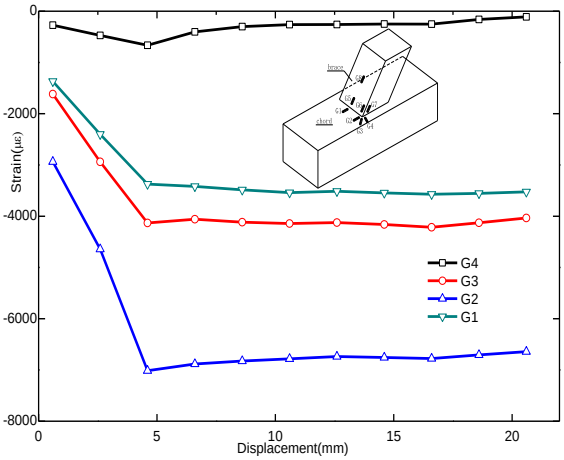

(c) J4 chord

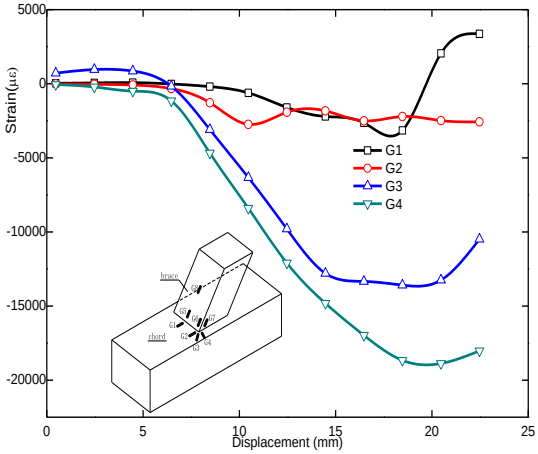

(d) J5 chord

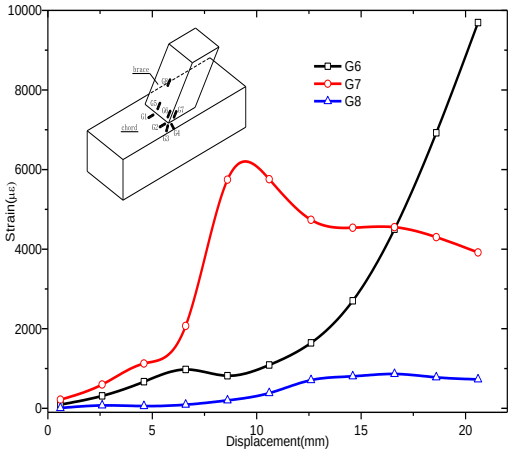

(e) J4 brace

Fig. 10 Chord face strain-displacement curve

and bump. After the peak load stage, load capacity lowered in a step fashion. The whole loading process represented the characteristics that the ductile stage of the joint of PBR was considerably longer than the joint without PBR.

3.2 Strain distribution curves

At the aspect of β's influence, test result showed that for the same angle θ the joint with PBR strength increased as the β raised up. At the aspect of θ's influence, for the same β the joint with PBR strength decreased as the θ increased.

Typical stress concentration spots' strain data were plotted in Fig. 10. For the joint J3 and J5 without PBR, at the early stage of loading, strain gauge of spot G1 was in compression due to the combination of bond and constraint by the side face of chord. As load increased, the top face of

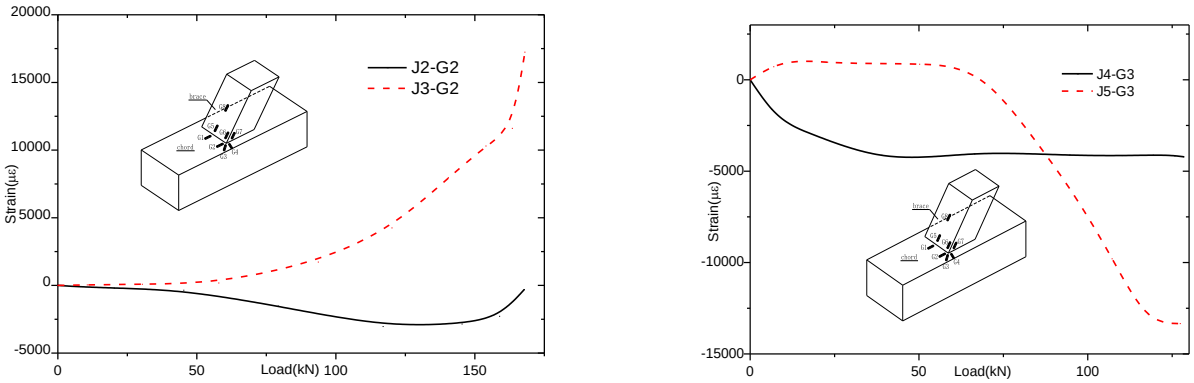

(a) Spot G2 (b) Spot G3

Fig. 11 Chord face strain-load curve

(a) β = 0.75 without PBR (b) β = 0.75 including PBR (c) β = 0.625 including PBR (d) β = 0.75 including PBR(θ = 90°)

Fig. 12 Typical failure modes of test specimens

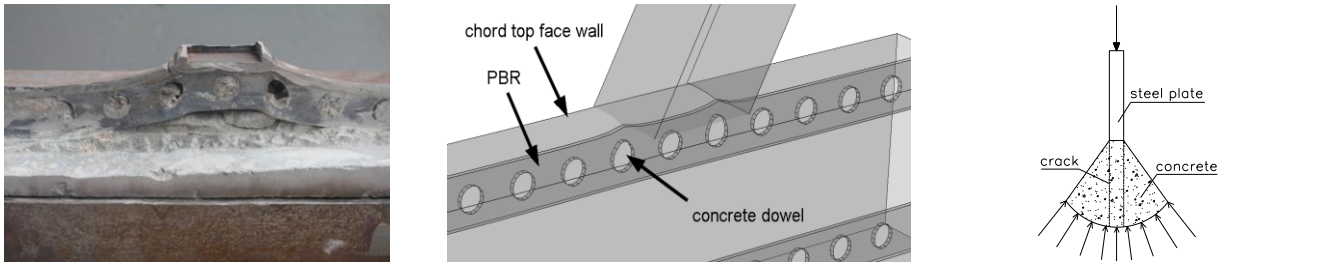

(a) Concrete dowel failure (b) PBR deformation demonstration (c) Concrete dowel failure mechanism

Fig. 13 Concrete dowel in PBR

chord bumped as a result of bond failure between steel and concrete. At the same time, spot G1's status changed from compression to tension. While for joint with PBR brace's stress concentration was still apparent as shown in Fig. 10(e), which was also validated by FEM analysis (Liu *et al.* 2015). In terms of joint with PBR, J2's spot G2 was in compression since the start of loading, while the same spot of J3 without PBR was in tension from the start and tensile strain ascended as the load increased (Fig. 11(a)). J4's spot G3 was in compression since the start of loading, while the same spot of J5 without PBR was in tension at the elastic stage (Fig. 11(b)). In general, stress states of these typical spots at the intersection of the chord and brace were mitigated and alternated from tension to compression due to the effect of PBR.

3.3 Ultimate tension test failure modes

For the joints without PBR (Fig. 12(a)), the failure mode presented by J3 was chord plastification. For the joints with PBR (Fig. 12(b)-(d)), at the early stage of loading, chord and brace nearly stayed un-deformed. As the load was approaching the ultimate point, the interaction between concrete and PBR in the joint made a continuous crack sound. When ultimate load was reached, chord face was observed a dramatic deformation with a sudden bang in the joint. The failure mode for the joints with PBR was observed to appear a compound of chord plastification and chord punching shear. Both modes co-existed during tension load. After failure of test joint, chord face and concrete were split as shown in Fig. 13(a). Observed from Fig. 13(a)-(b), concrete dowel under the brace cracked and PBR went through large deformation. Concrete dowel was in a state as shown in Fig. 13(c), in which the concrete through the hole was torn into failure by steel plate.

3.4 Fatigue test

Table 5 summarized the fatigue test result, in which N_1 and N_2 stood for cycles while first visible crack and fatigue

failure respectively. For J14 without PBR, initial fatigue crack took place in the intersection between chord and brace as shown in Fig. 14(a), which was the typical stress concentration spot for RHS joint. Fatigue crack tip developed along the weld of intersection. The stiffness of the joint degraded rapidly while fatigue crack propagated, which was demonstrated by N_2/N_1 (1.01) in Table 5. In comparison with J15 with PBR, the initial visible crack took place in the chord face which was welded to the side wall (Fig. 16(a)). After the propagation of the fatigue crack length reaching about 7-8 cm as shown in Figs. 15(b) and 16(b), it became steady for thousands of cycles. As the cycles increased, the fatigue crack tip continued to propagate to the intersection between the chord and brace (Fig. 16(c)). Till the crack became a through-thickness line around the corner, the joint lost strength completely (Fig.

(a) J14 N = 131449

(b) J14 N = 133265

Fig. 14 J14 fatigue crack propagation

Table 5 Fatigue test result

No.	N_1 (first visible crack, unit:cycle)	N_2 (fatigue failure, unit:cycle)	N_2/N_1	First visible crack position
J13	854096	984601	1.15	Chord
J14	131449	133265	1.01	Intersection between chord and brace
J15	1258158	1346168	1.07	Chord

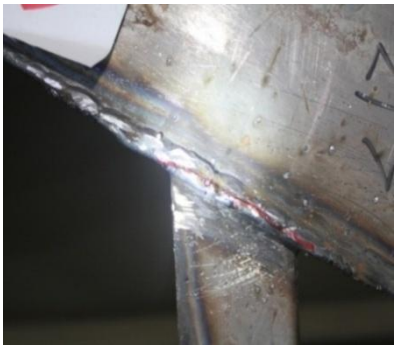

(a) J15 N = 1280056

(b) J15 N = 1284486

(c) J15 N = 1291997

(d) J15 N = 1318547

(e) J15 N = 1331136

(f) J15 N = 1341940

Fig. 15 J15 Fatigue crack propagation

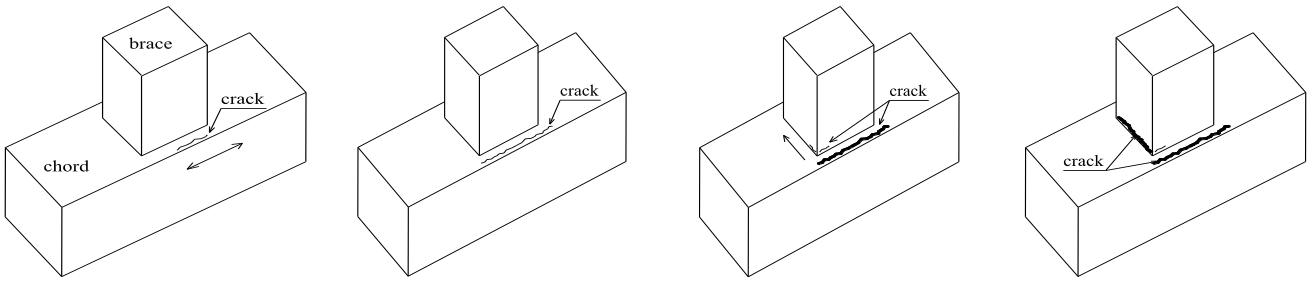

(a) I (b) II (c) III (d) IV

Fig. 16 Fatigue crack growth path of joint with PBR

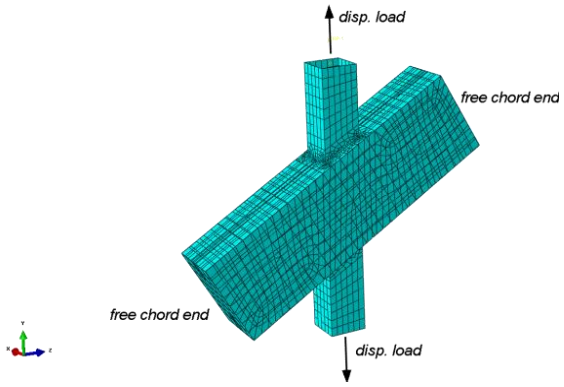

Fig. 17 FEM boundary condition

15(f) and 16(d)).

It was proved that typical stress concentration spot of HS joint was the intersection between brace and chord where FJ-2' initial crack took place (Vanwingerde 1992). However, it didn't apply to the CRHS joint with PBR. It was the PBR's effect which changed the chord face stress state. With PBR, the corner stress concentration was mitigated, while governing spot changed to the intersection between chord top face and side wall highlighted in Fig. 16(a), where weld was in tension and it was affected by the concrete in chord. This spot was in a complicated stress state. From the fatigue failure mode observed in test, PBR could significantly improve the fatigue life of CRHS joint.

4. Finite element verification

Analytic models of specimens were established by FEM program ABAQUS 12.0. The concrete material constitution adopted the model from GB50010-2010, while the steel material took Von Mise yield criterion with isotropic hardening as its constitutive model. The true stress-true strain relationship derived from coupon test was utilized as input. In terms of interaction, concrete and steel were set as friction interaction, PBR was embedded in concrete using EMBED method in ABAQUS (2012). A displacement-controlled load was imposed on the brace end and the chord end was free as shown in Fig. 17. Steel joint element type was reduced integration shell element (S4R). Concrete and PBR element type were reduced integration solid element (C3D8R). Test joints J2, J4 and J8 were picked as FEM verification cases. FEM ultimate tension capacity and deformation were compared to test results as shown in Figs. 18-19, which was in a good accordance with test result. Since PBR was simulated as embedded element in concrete and connected with chord, the elastic stiffness of joint appeared a little higher than test. Around the peak load, the dowel failed and PBR element yielded constantly in FEM which leaded to a fluctuation in the load-displacement curve as shown in Fig. 18. Another point should be noted, as shown in Figs. 20-21, the chord face shear plastic strain and maximum principal strain both occurred around the intersection of the joint. The phenomenon just explains the role of PBR inside the joint which stiffens the joint through

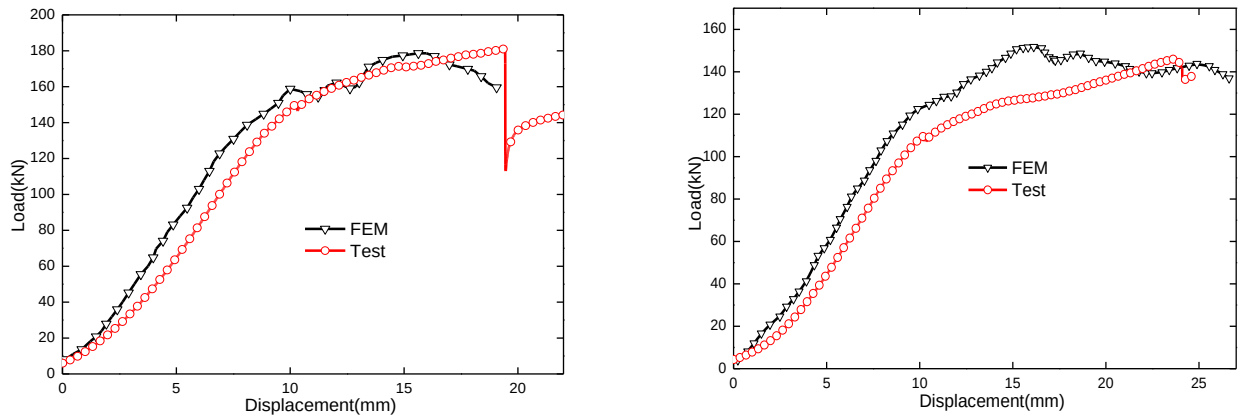

(a) J2 (b) J4

Fig. 18 Experimental and FEM comparison of load-displacement curves

(a) J2 FEM deformation (b) J2 test result

Fig. 19 J2 deformation comparison

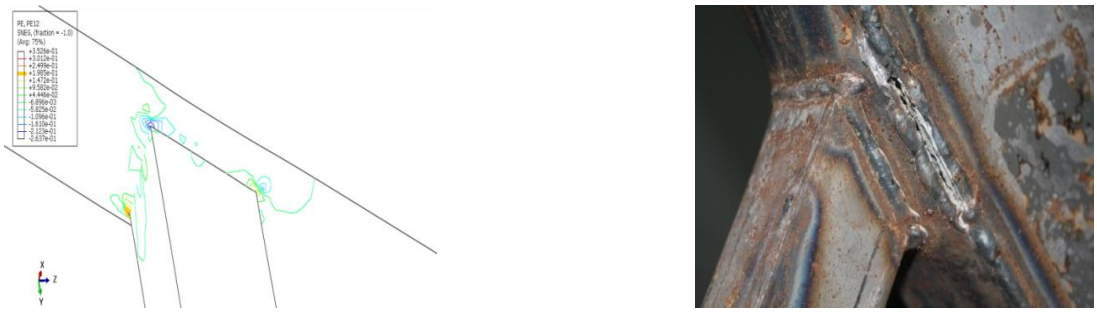

(a) FEM shear strain (b) Test result

Fig. 20 J4 chord shear strain against failure mode

(a) FEM maximum principal strain (b) Test result

Fig. 21 J8 chord maximum principal strain against failure mode

the concrete dowel between PBR's hole and concrete. Since the concrete dowel's effect, the failure mode of CRHS joint with PBR under tension is a combination of punching shear failure and chord plastification failure.

5. Effects of PBR and other influential factors

According to the test result, the tension strength of CRHS joint's with PBR has a significant relevance with the interaction between PBR and concrete besides the contributions of common factors such as β, θ, etc. As shown in Fig. 22(a), under tension loading, the core of the joint underwent large deformation, the concrete dowel of PBR failed in the core range, outside the core domain the PBR nearly remained as it was. In another word, the PBR influence to the CRHS joint ultimate tension capacity mainly makes effects in the core domain, which is named as PBR effective length hereafter.

As for the fatigue performance, fatigue crack inside the chord only propagated in the PBR effective length both in concrete and PBR itself as shown in Figs. 22(b)-(c). Another critical aspect affecting the fatigue life of CRHS joint was weld. Based on the propagation of fatigue crack presented in Fig. 16, the weld of chord wall face for large-scale truss should be serious treated. Penetration weld of at least 60% plate thickness is recommended for the fatigue durability.

6. Conclusions

Ultimate and fatigue experimental investigation were conducted in this study on CRHS X joints with PBR under

(a) PBR effective length

(b) Fatigue crack in concrete

(c) Fatigue crack in PBR

Fig. 22 PBR effective length

tension. Some conclusions can be drawn from the test results as follows:

- As for $\beta \leq 0.75$ joint, the ultimate tension strength of CRHS X joints could be considerably enhanced by PBR in chord. The ductility of the CRHS joint with PBR is also improved.
- The CRHS joint with PBR presents a combination failure mode under tension, which is consisted of punching shear and chord plastification. The mechanism of this compound failure mode has been found owing to the dowel formed by PBR's hole and concrete.
- As for CRHS joint with PBR, typical stress concentration area has been substantially mitigated than the joint without PBR. Observed from fatigue test, fatigue crack has initiated from the weld toe of chord side face and top face. Fatigue life after crack of CRHS joint with PBR is much longer than that without PBR.
- By splitting the failed test specimens, PBR inside chord has been found to function in an effective length, in this length dowel cracks and PBR deforms intensively. Far from the effective length, PBR rarely deforms.

Further research of the parametric analysis for CRHS joint with PBR under tension is recommended to learn the contribution of PBR stiffening effect and to propose the strength equation. Also chord axial tension load could be considered in parametric analysis, which has not been included in this test since its limited device capacity.

Acknowledgments

This paper was supported by the National Natural Science Foundation of China (Contract No. 51378068), Research Fund of Transportation Construction in West China (Contract No.2013318812410).

References

ABAQUS (2012), Abaqus user's manual; Version 6.12, Dassault Systems.

Ahn, J.H., Lee, C.G., Won, J.H. and Kim, S.H. (2010), "Shear resistance of the perfobond-rib shear connector depending on concrete strength and rib arrangement", *J. Constr. Steel Res.*, **66**(10), 1295-1307.

Baik, B., Yamada, K. and Ishikawa, T. (2011), "Fatigue crack propagation analysis for welded joint subjected to bending", *Int. J. Fatigue*, **33**(5), 746-758.

Cândido-Martins, J.P.S., Costa-Neves, L.F. and Vellasco, P.C.G.D.S. (2010), "Experimental evaluation of the structural response of perfobond shear connectors", *Eng. Struct.*, **32**(8), 1976-1985.

Cui, M.J. and Shao, Y.B. (2015), "Residual static strength of cracked concrete-filled circular steel tubular (CFCST) T-joint", *Steel Compos. Struct., Int. J.*, **18**(4), 1045-1062.

Feldmann, M., Pak, D., Kopp, M., Schillo, N., Hegger, J. and Gallwoszus, J. (2015), "Design of composite dowels as shear connectors according to the German technical approval", In: *Economical Bridge Solutions based on Innovative Composite Dowels and Integrated Abutments*, pp. 57-71.

Gallwoszus, J. and Classen, M. (2015), "Ermüdung von Verbunddübelleisten in UHPC unter zyklischer Pull-out-Beanspruchung", *Bautechnik*, **92**(7), 509-521. [In German]

Hanswille, G. (2011), "Composite bridges in Germany designed according to Eurocode 4-2", *Proceedings of the 6th International Conference on Composite Construction in Steel and Concrete*, Tabernash, CO, USA, July, pp. 391-405.

Liu, Y., Xiong, Z., Luo, Y., Cheng, G., Liu, G. and Yang, J. (2015), "Double-composite rectangular truss bridge and its joint analysis", *J. Traffic Transp. Eng.* (English Ed.), **2**(4), 249-257.

Machacek, J. and Cudejko, M. (2009), "Longitudinal shear in

composite steel and concrete trusses", *Eng. Struct.*, **31**(6), 1313-1320.
Packer, J.A. (1995), "Concrete-filled HSS connections", *J. Struct. Eng.*, **121**(3), 458-467.
Packer, J.A., Zhao, X.L., Vegte, G.J.V.D. and Wardenier, J. (2010), "Current static design guidance for hollow-section joints", *Struct. Build.*, **163**(6), 361-373.
Sakai, Y., Hosaka, T., Isoe, A., Ichikawa, A. and Mitsuki, K. (2004), "Experiments on concrete filled and reinforced tubular K-joints of truss girder", *J. Constr. Steel Res.*, **60**(3), 683-699.
Schumacher, A. and Nussbaumer, A. (2006), "Experimental study on the fatigue behaviour of welded tubular K-joints for bridges", *Eng. Struct.*, **28**(5), 745-755.
Schumacher, A., Borges, L.C. and Nussbaumer, A. (2009), "A critical examination of the size effect correction for welded steel tubular joints", *Int. J. Fatigue*, **31**(8), 1422-1433.
Seidl, G., Stambuk, M., Lorenc, W., Kołakowski, T. and Petzek, E. (2013), "Wirtschaftliche Verbundbauweisen im Brückenbau–Bauweisen mit Verbunddübelleisten", *Stahlbau*, **82**(7), 510-521. [In German]
Tue, N.V. and Küchler, M. (2006), "Knotengestaltung hybrider Fachwerkkonstruktionen–Entwicklung neuartiger Tragwerks-konzepte unter Verwendung von Ultrahochleistungsbeton (UHFB)", *Bautechnik*, **83**(5), 315-324. [In German]
Vanwingerde, A.M. (1992), "The fatigue behaviour of T- and X-joints made of square hollow sections", Ph.D. Dissertation; Delft University of Technology, Netherlands.
Xiao, Z.G., Chen, T. and Zhao, X.L. (2012), "Fatigue strength evaluation of transverse fillet welded joints subjected to bending loads", *Int. J. Fatigue*, **38**(38), 57-64.
Xiong, Z., Liu, Y., Zhang, N. and Song, S. (2014), "Structural performance of concrete-filled rectangular steel tubular joints with Perfobond Rib in bridges using damage model", *ASCE Geotechnical Special Publication*, **253**, 46-53.
Zheng, S., Liu, Y., Yoda, T. and Lin, W. (2016), "Shear behavior and analytical model of perfobond connectors", *Steel Compos. Struct., Int. J.*, **20**(1), 71-89.

BU

Nomenclature

b_0	external width of RHS chord
b_1	external width of RHS brace (perpendicular to the plane of the joint)
f_{y0}	yield stress of the chord
h_0	external depth of RHS chord
h_1	external depth of RHS brace
N_u	ultimate joint capacity based on the load in brace
N_1	Cyclic while first visible crack
$P_{\max}$	Maximum sine wave fatigue load
PBL	Perfobond Leister in the slab
RHS	Rectangular hollow section
β	width ratio between brace and the chord
θ	inclined angle between brace member and the chord
t_0	thickness of a hollow section chord
t_1	thickness of a hollow section brace
Δ_u	Corresponding displacement at the peak load
R	Stress ratio
N_2	Cyclic while fatigue failure
$P_{\min}$	minimum sine wave fatigue load
PBR	Perfobond Leister rib in joint
CRHS	Concrete-filled rectangular hollow section